Supplemental Information

"Water-in-salt" Polymer Electrolyte for Li-ion Batteries

Jiaxun Zhang[a‡], Chunyu Cui[a‡], Peng-Fei Wang[a‡], Qin Li[a], Long Chen[a], Fudong Han[a], Ting Jin[a], Sufu Liu[a], Hema Choudhary[a], Srinivasa R. Raghavan[a], Nico Eidson[ab], Arthur von Cresce[b], Lin Ma[b], Jasim Uddin[c], Dan Addison[c], Chongyin Yang[a*], Chunsheng Wang[ad*]

[a]. Department of Chemical and Biomolecular Engineering, University of Maryland, College Park, MD 20742, USA

[b]. Department Electrochemistry Branch, Sensor and Electron Devices Directorate, Power and Energy Division, US Army Research Laboratory, Adelphi, MD 20783, USA

[c]. Liox Power, Inc., Pasadena, CA, 90065, USA

[d]. Department of Chemistry and Biochemistry, University of Maryland, College Park, MD 20742, USA

‡ These authors contributed equally.

* Corresponding author.

Email: cswang@umd.edu, cyyang@umd.edu

Fabrication of crosslinked solid-state aqueous polymer electrolytes

Methacrylic based solid-state aqueous polymer electrolyte (SAPE) was prepared by in-situ solidification of a precursor solution on the $LiMn_2O_4$ cathode electrode.[1] The optimized aqueous polymer electrolyte is obtained by mixing the as-blended monomer solution with aqueous WiSE. BEMA (Bisphenol A ethoxylate dimethacrylate, M_n = 1700), PEGMA (Poly(ethylene glycol) methyl ether methacrylate, M_n = 500), HMPP (2-Hydroxy-2-methylpropiophenone, M_w = 164.2), were purchased from Sigma Aldrich. (M_n is number-average molecular weight, M_w is molecular weight)

The optimal composition of monomers shown below:

Table 1. The detailed weight ratio of each component in the electrolyte system.

Components (wt%)	LiTFSI	Pyr13-TFSI	LiOTf	BEMA	PEGMA	HMPP	H_2O
11m SAPE	63.7 %	0	10.2 %	1.54 %	13.55 %	0.31 %	10.7 %
12m SAPE	31 %	42.4 %	5.8 %	1.54 %	13.55 %	0.31 %	5.4 %

The precursor solution was polymerized under the UV light (IntelliRay 600) for 90 s with a transparent polypropylene sheet covered on the surface. All procedures were carried out in air condition for the advantage of aqueous electrolyte. The crosslinking degrees of 11m and 12m SAPE is 95.4 % and 93.8 % respectively. (relative error = ± 1%)

Ionic conductivity measurement of WiBS aqueous electrolytes and SAPE

The ionic conductivity was measured with electrochemical impedance spectroscopy (EIS) using the Solartron 1260 equipped with a 1287 Electrochemical Interface (Solatron Metrology, UK). The conductivity cell constants were predetermined using 0.01M aqueous KCl standard solution at room temperature.

The EIS of SAPE was measured with Gamry electrochemical instruments, coin cell was assembled with two stainless steel as electrode, the resistance of the electrolyte (R_b) from the high frequency intercept of the fitted impedance spectrum on the Z_{re} axis. The ionic conductivity, σ in S cm^{-1}, can be calculated from[2]

$$\sigma = \frac{L}{A * R_b}$$

Where L is the thickness (cm) and A represents the area of the electrolyte film (cm^2).

Rhegological experiments

The rheological experiments were performed on an AR2000 stress controlled rheometer (TA Instrument, Newark, DE).[3] Samples were run at 25 °C on the polymer discs (20 mm diameter, 1 mm height) relevant to various compositions. Dynamic frequency spectra were obtained in the linear viscoelastic regime of each sample as determined by dynamic stress-sweep experiments.

Preparation of anode passivation layer

PEO (MW = 1,000,000, Sigma Aldrich) was mixed with LiTFSI (Tokyo Chemical Industry), KOH (Sigma Aldrich) with the weight ratio of 0.55:0.25:0.2.The Mixture was dissolved in Methanol (Sigma, Aldrich) and heated at 70 °C for 2 hours. Then the gel-like passivation solution was casting on the $Li_4Ti_5O_{12}$ anode electrode by doctor blade and followed by drying on a hot stage at 60 °C for 48 hours under argon atmosphere to eliminate the solvent.

Preparation of flexible electrode and coating of electrolyte on electrode

The flexible substrates were prepared by coating Titanium current collector (0.5 μm thick) on kapton films (75 μm thick) with e-beam evaporation. The $LiMn_2O_4$ cathode and $Li_4Ti_5O_{12}$ anode electrodes were prepared by mixing 90% active material, 5% carbon black, and 5% polyvinylidene fluoride (PVDF) in Nmethylpyrrolidinone (NMP) and the slurry mixture was then coated on the surface of Titanium current collector. The electrodes were vacuum-dried at 100°C for 24 h. The mass loading of LMO cathode is around 4.6 mg cm^{-2}, the mass loading of LTO cathode is around 2.8 mg cm^{-2}.

First, we coated the LMO cathode with the SAPE precursor solution, and then the SAPE precursor coated LMO electrode was UV curved for 90 secs forming aqueous polymer electrolyte coated LMO cathode. The in-situ cross-linked electrolyte on electrode ensured a tight contact between electrolyte and LMO electrodes.

Electrode preparation and Electrochemical Measurements

The $LiMn_2O_4$ cathode and $Li_4Ti_5O_{12}$ anode electrodes were prepared by mixing 90% active material, 5% carbon black, and 5% polyvinylidene fluoride (PVDF) in 1-methyl-2-pyrrolidinone (NMP) and the slurry mixture was then coated on Al foil. After coating, the electrodes were dried at 80 °C for 12 hours to remove the solvent before pressing. The electrodes were cut into 2 cm^2

sheets, vacuum-dried at 100 °C for 24 h, and weighed before assembly. The mass loading of LMO cathode is around 4.6 mg cm^{-2}, the mass loading of LTO cathode is around 2.8 mg cm^{-2}. The galvanostatic charge/discharge measurements were performed using Land BT2000 battery test system (Wuhan, China) at room temperature. The Cyclic voltammetry (CV) tests of electrode materials was carried out with three-electrode system using activated carbon as counter and Ag/AgCl as reference electrodes, respectively. The linear sweep voltammetry (LSV) tests of electrolytes was carried out with three-electrode system using inactive current collector (Titanium foil or Aluminum foil) as working electrode, activated carbon as counter and Ag/AgCl as reference electrodes, respectively. The CV and LSV measurements were carried out on a Gamry electrochemical instruments. The Chronoamperometry tests of electrolytes was carried out with three-electrode system using inactive current collector (Titanium foil or Aluminum foil) as working electrode, activated carbon as counter and Ag/AgCl as reference electrodes, respectively. The potentiostatic measurements were carried out on a Gamry electrochemical instruments.

In-situ cell pressure and Mass spectra test

The In-situ cell pressure experiments were carried out in a specially designed hermetically sealed cell fixture with known volume (V_{cell} = 89.30 cm^3). This two electrode sealed cell consisted of a pressure sensor (OMEGADYNE, MODEL NO. PX329-030A5V, 0-30 PSI Range) and a prime/purge valve (Valco Instruments) to easily evacuate internal gases and fill again with argon or helium. The valve can also easily be connected to a mass spectrometer (Pfeiffer HiCube 80 Eco Turbo Pumping Station, Includes HiPace 80 Turbo Pump, DN 63 CF-F) together with Sanford Residual Gas Analyzer (SRS RGA Series up to 100 amu). The in situ pressure change (ΔP) during cycling at isothermal condition (using ΔPV_{cell} = nRT) together with RGA data (up to 100 amu) allowed us to precisely analyze, *both qualitatively and quantitatively*, the evolved gases. The fixture was leak-tested with helium gas at 30 °C for an overnight before each experiment. RGA data was taken before and after the cell cycling and overlaid them to see if any new gas was generated during the cycling or not.

Material Characterizations

The morphology of the sample was performed by using SEM (Hitachi SU-70). Fourier transform infrared spectroscopy (FTIR) was performed with a Nicolet 6700 spectrometer instrument and a Golden Gate single reflection monolithic diamond attenuated total reflection (ATR) sample cell. Raman measurements were performed on a Horiba Jobin Yvon Labram Aramis using a 532 nm diode-pumped solid-state laser. X-ray photoelectron spectroscopy (XPS) was conducted on a high sensitivity Kratos AXIS 165 X-ray photoelectron spectrometer with Al Kα radiation. The ex situ tested electrodes were retrieved from the full cells, then soaked in Dimethyl ether (DME, Sigma Aldrich) for 12 hours to remove all remaining SAPE and PEO passivation layer on LTO surface. The whole process was carried in pure Ar filled glove box to eliminate contamination.
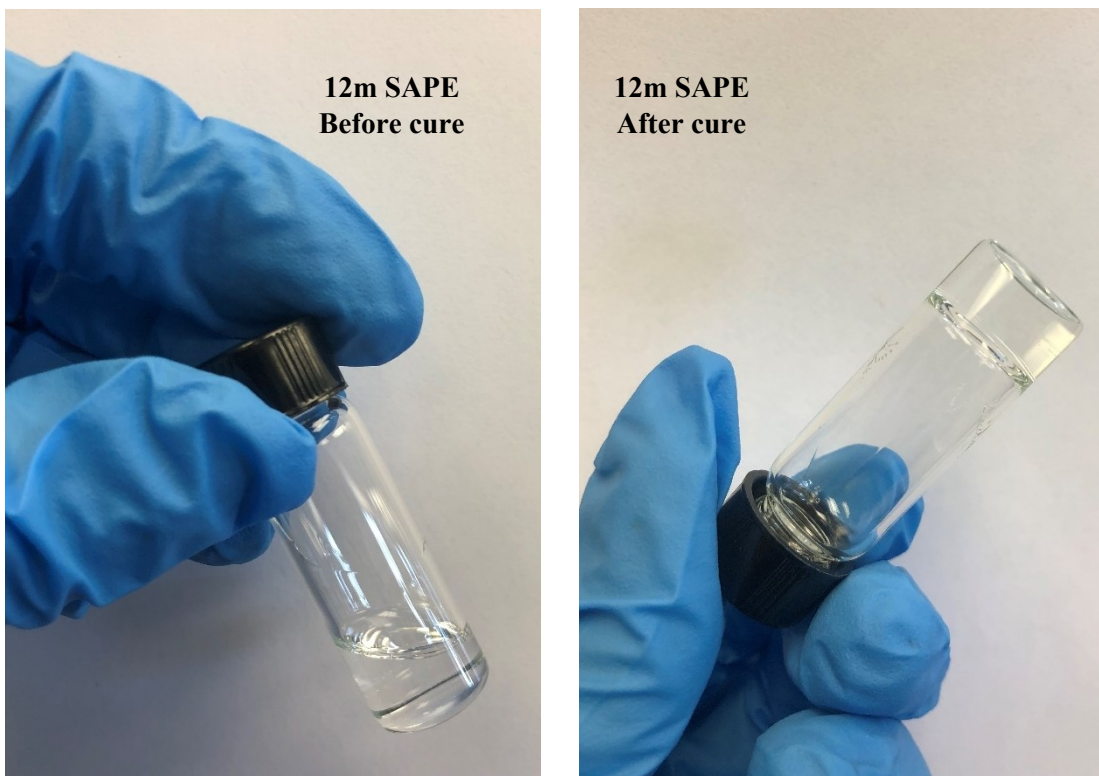
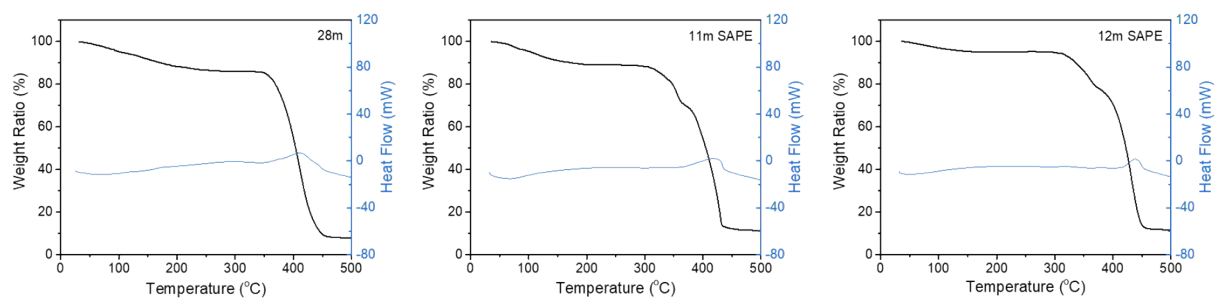**Figure S1**. Photograph of the 12m SAPE solution before UV-curing and after UV-curing.

Figure S2. Differential scanning calorimetry (DSC) scans of 28m WiSE, 11m SAPE and 12m SAPE.
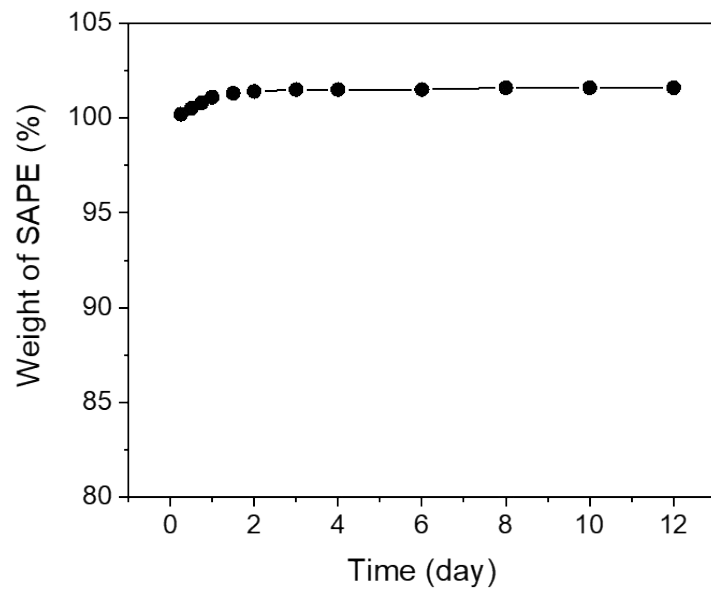
Figure S3. The weight retention rate of 12m SAPE in the air at room temperature (relative humidity of 60% is test during the experiment period)
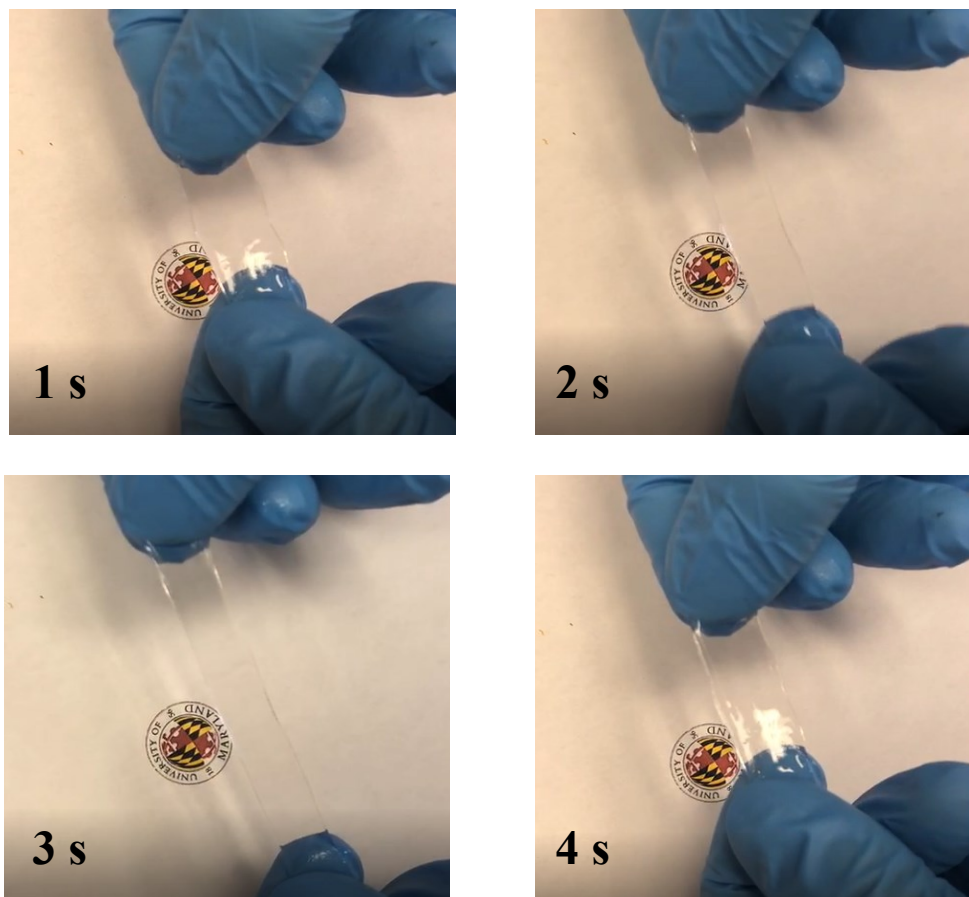

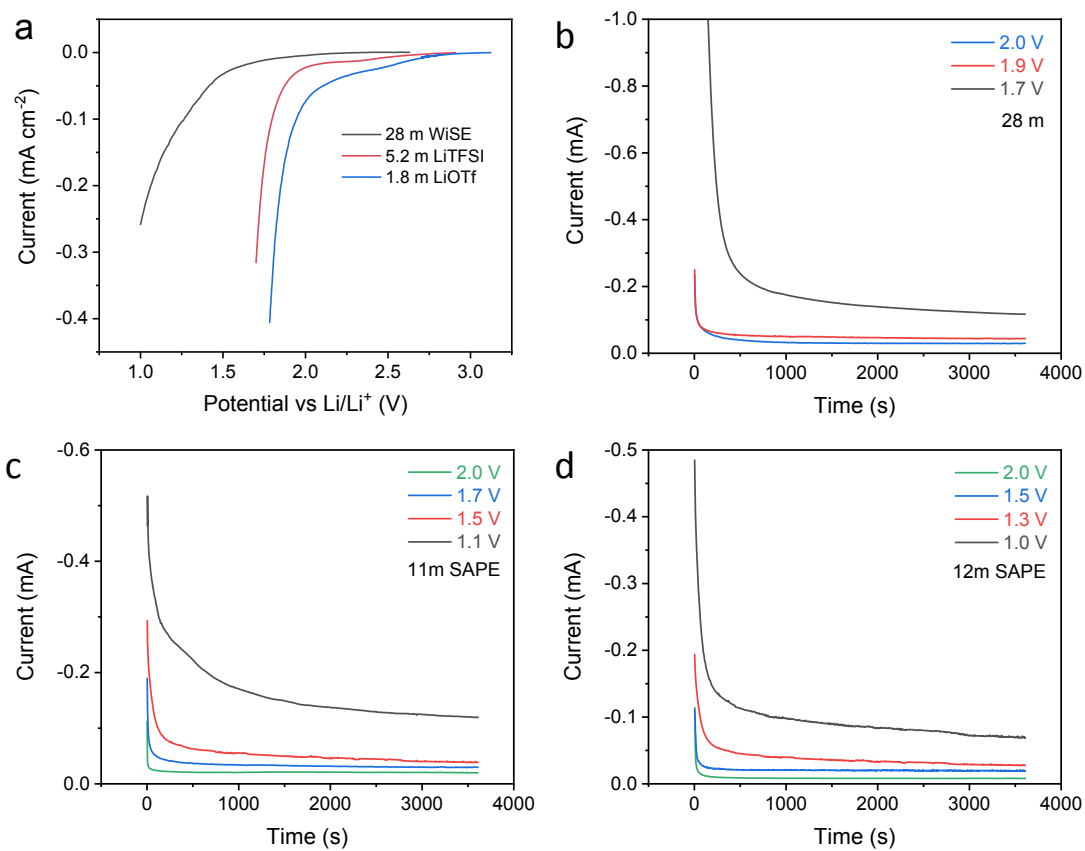**Figure S4**. Photograph of SAPE under stretching.

Figure S5. (a) The linear sweep voltammetry of 5.2m LiTFSI, 1.8m LiOTf and 28m WiSE at scanning rate of 0.1 mV s^{-1}. And current-time curve of Al electrodes at different potentials in 28m WiSE (b), 11m SAPE (c) and 12m SAPE electrolytes (d)
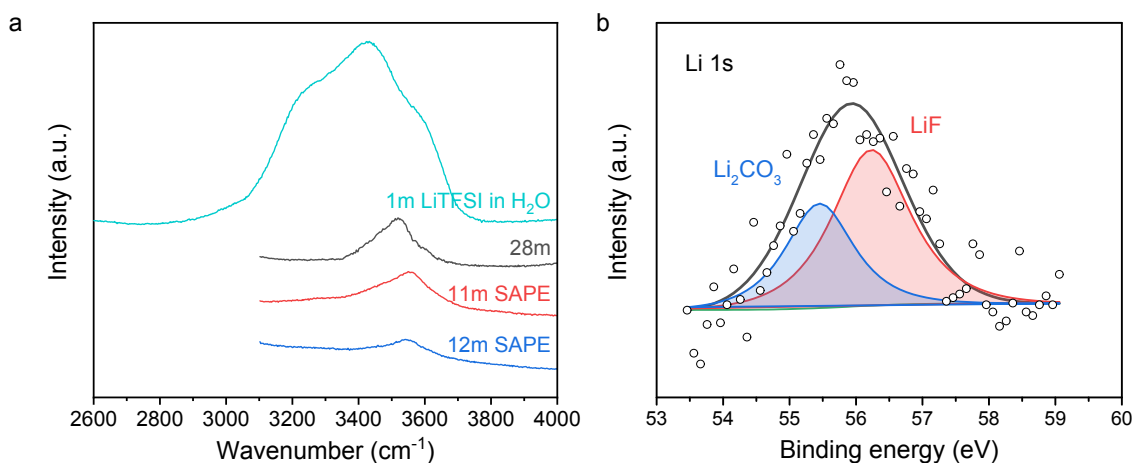

Figure S6. (a) Raman spectra of 28mWiSE, 11m SAPE and 12m SAPE. (b) Li 1s XPS spectra of the LTO anode after 20 cycles with 12m SAPE@SPE as electrolyte.
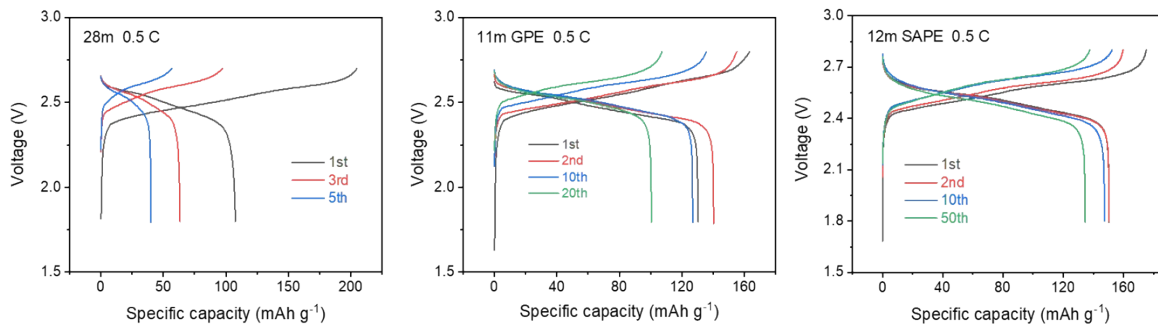
Figure S7. The typical voltage profile of LMO/LTO full cell with different electrolytes at constant current of 0.5C.
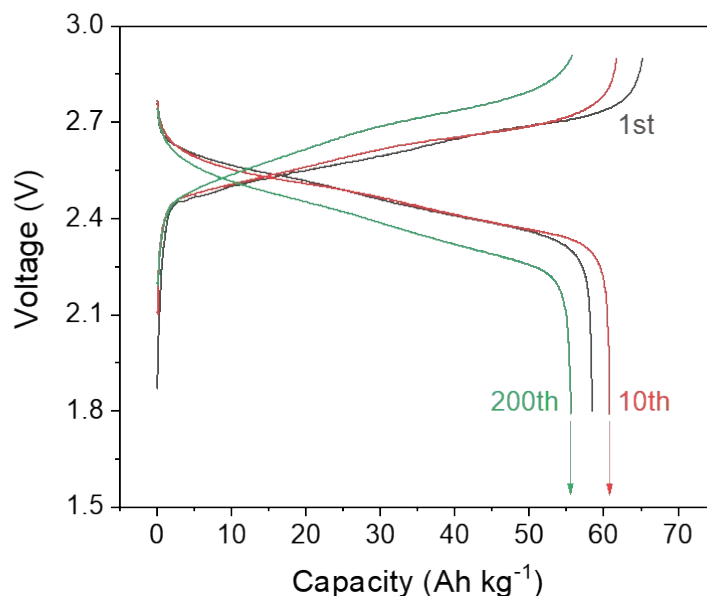

Figure S8. The typical voltage profile of LMO/LTO full cell at constant current of 0.5C. (Based on the mass of LMO and LTO)

In this manuscript, our electrolyte 12m SAPE is composed of LiTFSI, Pyr13-TFSI, LiOTf, H_2O and monomers. From the aspect of inorganic/organic composition ratio, we have done a series of optimization test on the monomers' ratio and Pyr_{13} TFSI's molar ratio.

Determination of the ratio of ionic liquid Pyr13-TFSI in the WIS electrolyte:

Firstly, we investigated the ratio of monomers and WiSE. To simplify the expression, we calculate the ratio of monomers and WiSE by weight and the different weight ratio of the two component was characterized as M-10, M-15, M-20 and M-25 (Shown in **Table S2**). The LMO//LTO full Li-ion cell with capacity ratio (LMO/LTO) of 1.14 and areal capacity of 0.5 mAh cm^{-2} is assembled to evaluate the electrochemical performance in above electrolytes. The cycling performances are presented in **Figure S9**. The ionic conductivity of M-10 electrolyte is 2.1 mS cm^{-1}, the discharge capacity is close to the theoretic value, while the Coulombic efficiency is not high enough. Thus, the discharge capacity is decay faster than the M-15 electrolyte (12m SAPE). With the increase of

polymer's weight ratio increase from 15% to 20% and 25%, the ionic conductivity decreased significantly. The discharge capacity of M-20 and M-25 is smaller than the M-15. Thus, the optimized polymer ratio is 15%, which is our result presented in the manuscript.

Table S2: Ionic conductivity of different monomers weight ratio electrolytes (M-10, M-15, M-20, M-25)

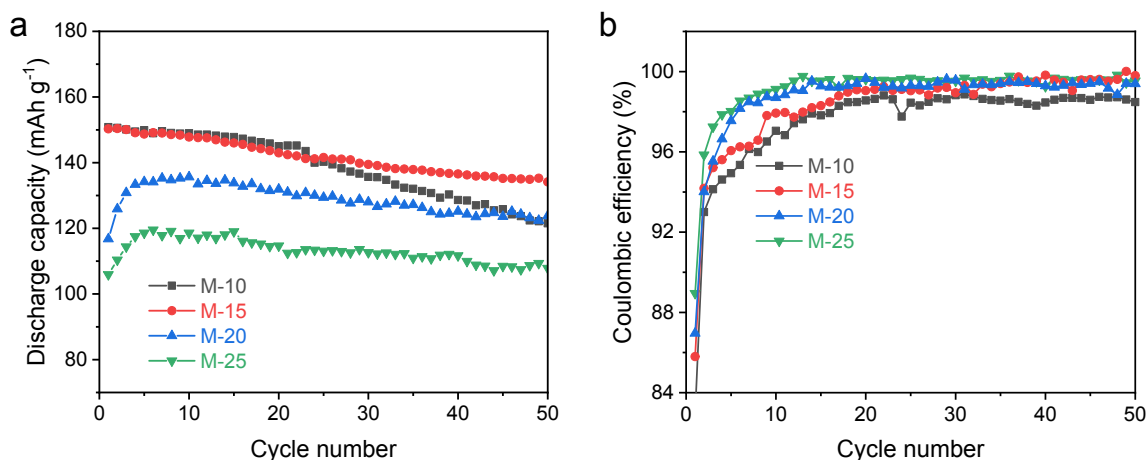| Weight Ratio (wt%)	Monomers (BEMA + PEGMA + HMPP)	WiSE (LiTFSI + Pyr13-TFSI + LiOTf + H2O)	Ionic conductivity (mS/cm) At 25 °C
M-10	10 %	90 %	2.1
M-15	15 %	85 %	1.7
M-20	20 %	80 %	1.1
M-25	25 %	75 %	0.6

Figure S9. Cycling stability (a) and Coulombic efficiency (b) of LMO//LTO full cell in different monomers weight ratio electrolytes (M-10, M-15, M-20, M-25) at 0.5C.

Determination of the ratio of ionic liquid Pyr13-TFSI in the WIS electrolyte:

Secondly, we investigated the effect of different molar ratio of ionic liquid Pyr13-TFSI in the solid state aqueous polymer electrolyte. Here, we set the weight ratio of monomers as 15 wt%. By mixing different molar of Pyr13-TFSI with 28m lithium salt in water, we can get different SAPE with varied Pyr13-TFSI ratio. To simplify the expression, we simplify the different molar ratio of Pyr13-TFSI in the electrolyte as P-5, P-10, P-20 and P-30 (Shown in **Table S3**)

The LMO//LTO full cell with capacity ratio (LMO/LTO) of 1.14 and areal capacity of 0.5 mAh cm^{-2} is assembled to evaluate the electrochemical performance in above electrolytes. The cycling performances are presented in **Figure S10**. The ionic conductivity of P-5 and P-10 electrolyte is 2.65 and 2.15 mS cm^{-1}, respectively. The discharge capacity of P-5 and P-10 is close to the theoretic value, while the Coulombic efficiency is not high enough. Thus, the discharge capacity is decay faster than the P-20 electrolyte (12m SAPE). With the increase of Pyr13-TFSI's molar

ratio increase from 20 m to 30 m, the ionic conductivity decreased. The discharge capacity of P-30 is smaller than P-20. Though the cycling stability of P-30 is better than P-20, the discharge capacity is not fully presented in the cycling process. The reason is the low ionic conductivity of electrolyte impede the transfer of ions in the electrolyte and the active materials in the electrode is not fully used in the beginning of cycling. Thus, the optimized ionic liquid Pyr13-TFSI's molar ratio is 20 m (12m SAPE), which is our result presented in the manuscript.

Table S3: Ionic conductivity of different molar ratio of Pyr13-TFSI in the electrolytes (P-10, P-10, P-20, P-30)

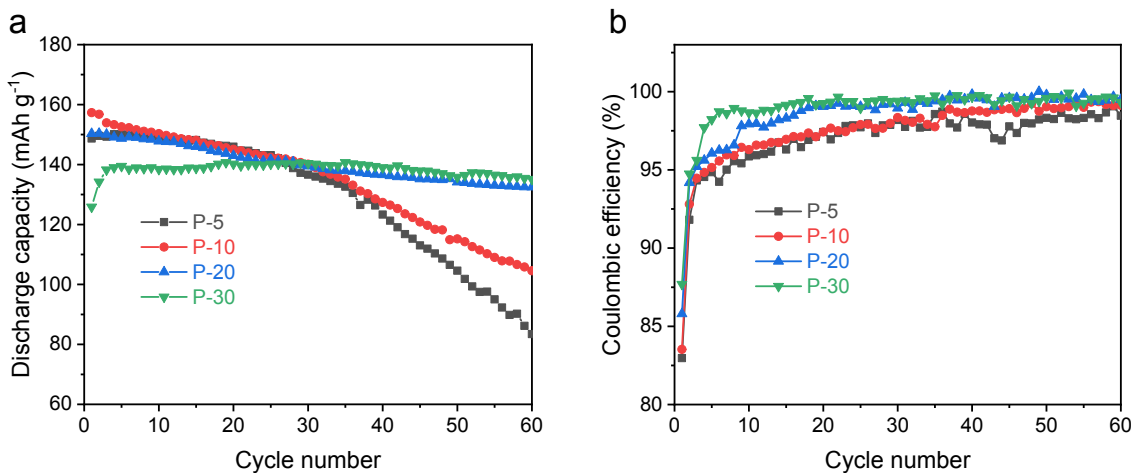| Number	Monomers (BEMA +PEGMA + HMPP)	21m LiTFSI + 7m LiOTf in 1 kg H_2O	Pyr13-TFSI (molar in 1 kg H_2O)	Ionic conductivity (mS/cm) At 25 °C
	15% (wt %)	85% (wt %)		
P-5	15 %	28m	5m	2.65
P-10	15 %	28m	10m	2.15
P-20	15 %	28m	20m	1.7
P-30	15 %	28m	30m	1.45

Figure S10. Cycling stability (a) and Coulombic efficiency (b) of LMO//LTO full cell in Pyr13-TFSI molar number electrolytes (P-5, P-10, P-20, P-30) at 0.5C.
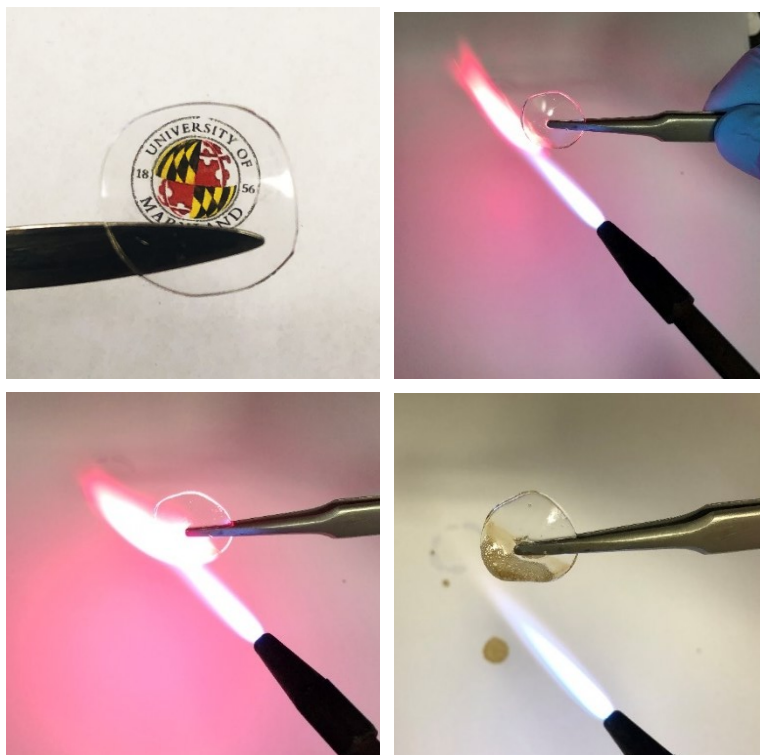
Figure S11. The flame tests of the 12m SAPE under the high-temperature Propane-Oxygen flame. The composition of LiPF$_6$-GPE in Video S2 is cross-linked solid polymer (10 wt% BEMA and 90 wt% PEGMA) absorbed in 1M LiPF6 EC/DMC for 24 h.
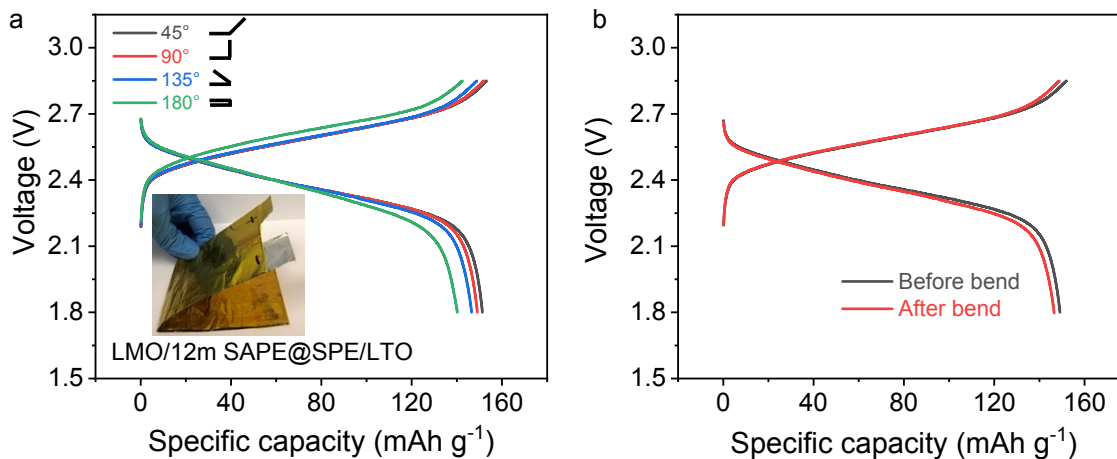

Figure S12. (a) The voltage profiles of LMO//LTO flexible battery with 12m SAPE@SPE electrolyte at 0.5 C under different bending angles: 45°, 90°, 135°, 180°. (b) The typical voltage profile of LMO/LTO flexible cell before bend and after 200 times bend.
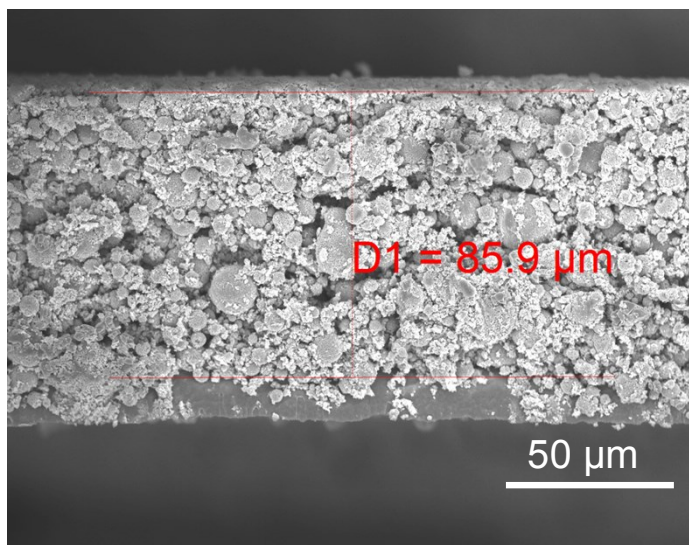
Figure S13. A pouch cell with capacity of 100 mA h.

Figure S14: Cross-section SEM image of composite LTO electrode with loading of 1.5 mA h cm^{-1}.
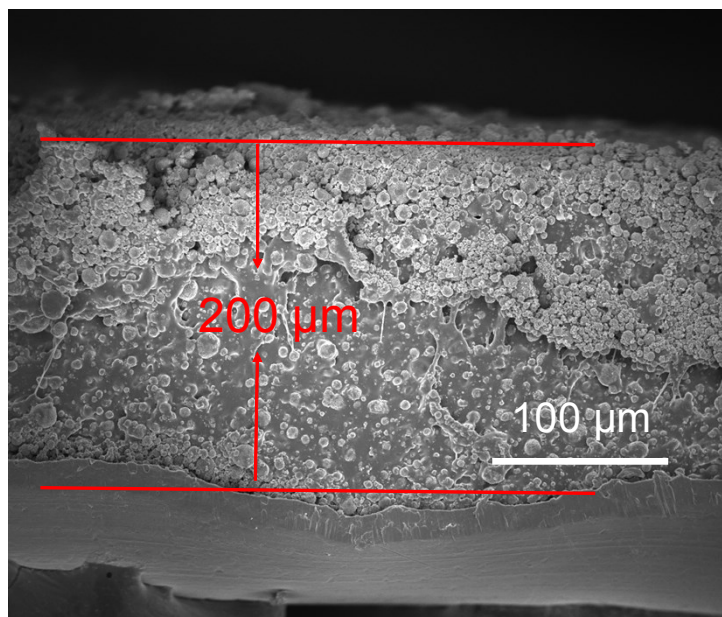
Figure S15. Cross-section SEM image of UV cured LTO-SAPE electrode.

Calculation of Coulombic efficiency of LMO/LTO full cell

The Coulombic efficiency of the LMO/LTO full cell can be calculated with the following method:

For example: The cathode/anode capacity ratio is 1.1:1, the Coulombic efficiency of cathode and anode was set as 100% and 99%, respectively. Here, we ignore the low Coulombic efficiency of the first several cycles, assume the Coulombic efficiency of cathode and anode is ideal. Also, we ignore the influence of electrolyte on CE. Thus, the capacity of the full cell presents in the first several cycle is the capacity of anode, the capacity of cathode decay 1% each cycle owing to the consume of lithium at anode. After 10 cycles, the extra capacity of cathode is exhausted, the capacity of the full cell will start to decline at an exponential rate. We can draw a schematic diagram to exhibit the process. After 30 cycles, the remained capacity of the cell is 81.8% of the initial capacity. The theoretical diagram of the above process is presented in **Figure S16**.
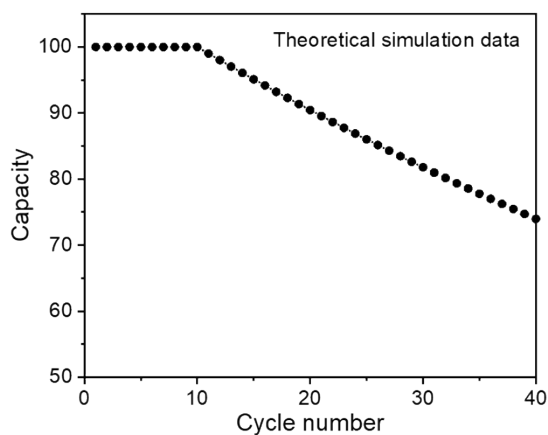

Figure S16. Schematic diagram of cycling stability under theoretical condition.

Herein, for the LMO//LTO full cell with 12m SAPE@SPE electrolyte at 0.5C. We can calculate the CE with the above method. As we mentioned, the excess capacity of cathode is 14% than capacity of anode. The CE of first cycle is 90.50 %, about 10% cathode capacity is consumed. The CE of next 4 cycle is less than 99 %, thus, the excess capacity of cathode is consumed completely in the first several cycles. Thus, the true CE of the full cell from 10 to 200 cycle can be calculated from the decay of discharge capacity. 155.2 mA h g^{-1} $_{(LTO)}$ is achieved at 10th cycle. 141.1 mA h g^{-1} $_{(LTO)}$ is achieved at 200th cycle. 90.9 % of the 10th cycle's capacity is retained after 190 cycles. Therefore, the CE from 10th cycle to 200th cycle is 99.95 %. (0.9995$^{\wedge 190}$ = 0.909). Similarly, the CE of LMO//LTO full cell with 12m SAPE@PEO-LiTFSI-KOH electrolyte at 1 C also can be calculated with this method.

References

1.   J. Nair, C. Gerbaldi, G. Meligrana, R. Bongiovanni, S. Bodoardo, N. Penazzi, P. Reale and V. Gentili, *Journal of Power Sources*, 2008, **178**, 751-757.

2.   S. Liang, W. Yan, X. Wu, Y. Zhang, Y. Zhu, H. Wang and Y. Wu, *Solid State Ionics*, 2018, **318**, 2-18.

3.   S. Gharazi, B. C. Zarket, K. C. DeMella and S. R. Raghavan, *ACS Appl Mater Interfaces*, 2018, **10**, 34664-34673.